International Journal of Fatigue 33 (2011) 948–958

Contents lists available at ScienceDirect

International Journal of Fatigue

journal homepage: www.elsevier.com/locate/ijfatigue

Multiaxial fatigue: An overview and some approximation models for life estimation

Ali Fatemi *, Nima Shamsaei

Mechanical, Industrial and Manufacturing Engineering Department, The University of Toledo, 2801 West Bancroft Street, Toledo, OH 43606, USA

ARTICLE INFO

Article history:
Received 29 September 2010
Received in revised form 13 December 2010
Accepted 1 January 2011
Available online 6 January 2011

Keywords:
Multiaxial fatigue
Damage mechanism
Non-proportional hardening
Mixed-mode crack growth
Life estimation

ABSTRACT

A brief overview of some important issues in multiaxial fatigue and life estimation is presented. These include damage mechanisms and damage quantification parameters, material constitutive response and non-proportional hardening, cycle counting and damage accumulation in variable amplitude loading, and mixed-mode crack growth. It is shown that capturing the correct damage mechanism is essential to develop a proper damage quantification parameter for robust multiaxial fatigue life estimation. Additional cyclic hardening of some materials under non-proportional multiaxial loading and its dependence on the load path as well as material microstructure is also discussed. It is argued that critical plane damage models with both stress and strain terms are most appropriate since they can reflect the material constitutive response under non-proportional loading. Importance of a proper cycle counting method to identify cycles in a variable amplitude load history, and capability of the linear cumulative damage rule to sum damage from the counted cycles are also discussed. As mixed-mode crack growth can constitute a significant portion of the total fatigue life, analysis of crack growth rates and correlations under combined stresses is presented. Several models as well as some simple approximations in capturing the aforementioned effects in multiaxial fatigue life estimations are also described. The approximation models include an estimation model for obtaining material non-proportional cyclic hardening coefficient, and a simple multiaxial fatigue life estimation model for steels based on hardness as the only required material property.

1. Introduction

Multiaxial loads, which can be in-phase (proportional) or out-of-phase (non-proportional), are common for many components and structures. Even under uniaxial loads multiaxial stresses often exist, although typically in-phase, for example due to geometric constraints at notches. Such multiaxial loads and stress states are frequently encountered in many industries, including automotive, aerospace, and power generation, among others.

The earliest works on multiaxial stress states, although under monotonic loading, relate to classical yield theories of Lame and Tresca in the late 19th century and von Mises in the early 20th century. While the first combined load testing is attributed to Lanza in 1886 [1], the first systematic study of multiaxial fatigue was conducted by Gough and Pollard in 1930s [2]. The bending–torsion data generated from the study of Gough and Pollard provided the basis for the models later proposed by Gough [3], Sines [4], and Findley [5] in the 1950s. Much of the early multiaxial fatigue work, however, related to high cycle fatigue and *S–N* analysis, where plastic strain is typically small or negligible.

Since these early works, much additional experimental as well as theoretical works on the challenging problem of multiaxial fatigue have been accomplished, particularly in the last four decades, with the advent of accurate multiaxial fatigue testing equipment. A series of international conferences and symposia have been dedicated to this topic in the last 30 years, including those in San Francisco – USA in 1982, Sheffield – UK in 1985, Stuttgart – Germany in 1989, San Diego – USA in 1991, St. German-en-Layne – France in 1994, Denver – USA in 1995, Cracow – Poland in 1997, Lisbon – Portugal in 2001, Berlin – Germany in 2004, Sheffield – UK in 2007, and Parma – Italy in 2010.

The results from these conferences and symposia have been published in proceedings, and some have been published as ASTM Special Technical Publications (STP 853, STP 1191, STP 1280, and STP 1387). SAE Fatigue Design and Evaluation Committee also had a multiaxial fatigue testing and analysis program in the 1980s and the 1990s, the results of which were published as SAE Advances in Engineering series (AE 14 and AE 28). A multiaxial fatigue book by Socie and Marquis [6] provides working knowledge of multiaxial fatigue damage processes and life estimation models, including illustrative examples.

The large amount of experimental data generated and research performed over the last four decades has significantly advanced the understanding of the complex issue of multiaxial fatigue.

* Corresponding author. Tel./fax: +1 419 530 8213.
E-mail address: afatemi@eng.utoledo.edu (A. Fatemi).

0142-1123/$ - see front matter © 2011 Elsevier Ltd. All rights reserved.
doi:10.1016/j.ijfatigue.2011.01.003

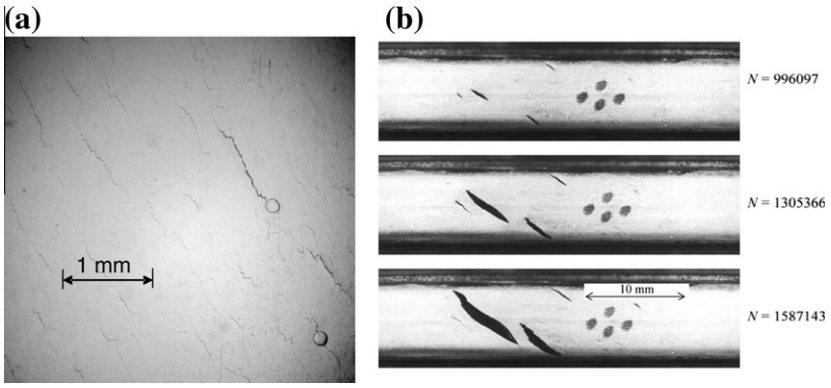

Fig. 1. Preferred cracking orientations observed for (a) 1050 normalized steel under in-phase axial–torsion loading, and (b) natural rubber under 90° out-of-phase axial–torsion loading.

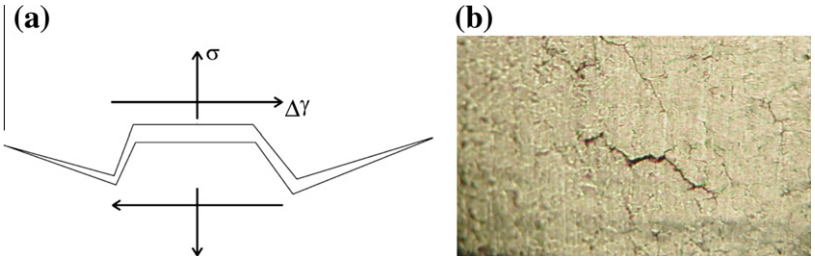

Fig. 2. Cracking mechanism for shear damage material [6] (a) and typical irregularly shaped fatigue crack (b).

However, as this challenging problem remains elusive, and due to its practical application significance, much additional research and development work is still needed for accurate and reliable evaluation of multiaxial fatigue design, life estimation, and failure assessment.

This paper is not intended to be a review paper, but rather, an overview sort of paper, where several important issues related to multiaxial fatigue are discussed. These include brief discussions of: (1) damage mechanisms, as they provide the basis for critical plane life evaluation approaches, (2) non-proportional hardening and constitutive behavior, since they can significantly affect fatigue behavior, (3) damage parameters and life estimation, as they are key ingredients of any life assessment methodology, (4) variable amplitude loading, cycle counting, and damage accumulation, due to their significant implications related to service loadings of many structures and components, and (5) mixed-mode crack growth, as it can constitute a significant portion of the total fatigue life. Some simple approximations for capturing some of these effects in multiaxial life estimation are also provided.

Although the scope of this paper is relatively broad, it is by no means comprehensive, as some other important effects such as notch behavior and elevated temperatures are not included. It should also be mentioned that much of the data and many of the models presented are based on or influenced by the author and his collaborators works in this area, and therefore, admittedly biased. As this is not a literature survey or review paper, many other works in this area, although significant, are not presented.

2. Damage mechanisms

Fatigue life generally consists of crack nucleation and crack growth. In ductile-behaving materials, cracks typically nucleate along slip systems, which are aligned with the maximum shear planes. In brittle-behaving materials, cracks often nucleate directly at discontinuities, such as inclusions and voids, although they can also nucleate in shear. Once cracks nucleate, their growth can be divided in two stages, stage I associated with micro-crack growth (i.e. early growth) along maximum shear planes, and stage II associated with crack growth along maximum tensile stress plane. Micro-crack growth life of ductile-behaving materials is typically dominated by stage I growth, while crack growth life of brittle-behaving materials is typically dominated by stage II growth.

Systematic investigation of cracking behavior under multiaxial loading by several investigators, including Socie and co-workers [7,8] and Brown and Miller [9,10], indicated that cracks nucleate and grow on preferred planes rather than with random orientation. The preferred orientation depends on the material and the state of loading. The preferred orientation of crack plane nucleation and growth has also been observed for non-metallic systems, such as in elastomers [11] with material structure very different from that of metals (i.e. polymer chains).

Examples of preferred crack plane nucleation and growth are shown in Fig. 1. Fig. 1a shows a large number of cracks in a normalized medium carbon steel under in-phase axial–torsion loading, where all the cracks are oriented along the maximum shear plane. Fig. 1b shows multiple cracks in natural rubber under 90° out-of-phase axial–torsion loading, where they are all along the same preferred orientation. These cracks continue to grow along the same direction with increasing number of loading cycles.

These observations have provided the physical basis for critical plane approaches to multiaxial fatigue. These approaches, which reflect the material damage mechanism, are based on either maximum shear failure plane, or maximum principal strain or stress failure plane. For the former case, the primary fatigue damage driving parameter is shear strain or stress, while for the latter case the primary damage driving parameter is the maximum principal stress or strain. For shear cracking mechanism materials, the stress normal to the cracking plane can have a secondary influence. This is because cracks typically grow in a zigzag or irregularly shaped

manner at the microscopic scale. A tensile normal stress opens the crack, reducing crack closure, and resulting in decreased fatigue life. In contrast, a compressive normal stress closes the crack, increasing crack closure and resulting in increased fatigue life. Fig. 2a shows schematic representation of shear cracking mechanism of an irregularly shaped crack and Fig. 2b shows a photo of a typical irregularly shaped fatigue crack.

In high hardness or brittle-behaving materials, even though high cycle fatigue cracks are typically observed to grow on the maximum principal stress or strain plane, the mode of failure may still be dominated by a shear mechanism in low and intermediate cycle fatigue regimes. This is due to the presence of plastic deformation which may exist at shorter lives. For example, torsion fatigue tests of case-hardened specimens of a medium carbon steel indicated surface cracking on the maximum shear plane in low cycle fatigue, a transition from shear to maximum principal plane in the intermediate life regime, and tensile failure mode in high cycle fatigue, as shown in Fig. 3 [12,13].

3. Non-proportional hardening and constitutive modelling

The principal directions of cyclic loading remain fixed in proportional multiaxial loading, whereas principal axes rotate in time for non-proportional multiaxial loading. Some materials exhibit strain hardening due to the non-proportionality of cyclic loading. This phenomenon was first observed by Taira et al. [14] and later explained by Lamba and Sidebottom [15] and Kanazawa et al. [16]. The additional hardening is attributed to the change in crystallographic slip planes due to the rotation of maximum shear plane and intersection of these planes under non-proportional loading.

The level of non-proportional cyclic hardening depends on the shape, sequence, and amplitude of the load path, as well as the microstructure of the material. Fig. 4 shows cyclic deformation behavior of two materials under proportional (in-phase) and non-proportional (90° out-of-phase) loadings. While the Ti alloy exhibits the same behavior under the two loadings [17], the stainless steel exhibits significant additional hardening under non-proportional loading [18,19].The maximum possible strain hardening usually results from 90° out-of-phase loading. Sensitivity of a material to non-proportional cyclic loading is commonly determined by non-proportional cyclic hardening coefficient, α, defined as:

$$\alpha = \frac{\bar{\sigma}_{OP}}{\bar{\sigma}_{IP}} - 1 \tag{1}$$

where $\bar{\sigma}_{OP}$ is 90° out-of-phase equivalent stress amplitude and $\bar{\sigma}_{IP}$ is in-phase equivalent stress amplitude at the same strain amplitude level.

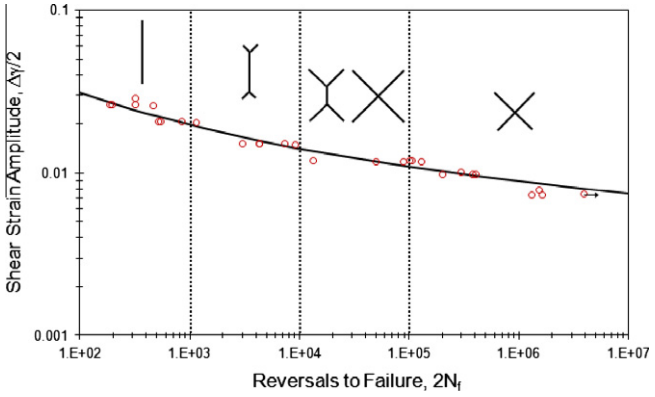

Fig. 3. Surface shear strain amplitude versus reversals to failure and cracking mode in torsion fatigue tests of 1050 steel case-hardened specimens [12,13].

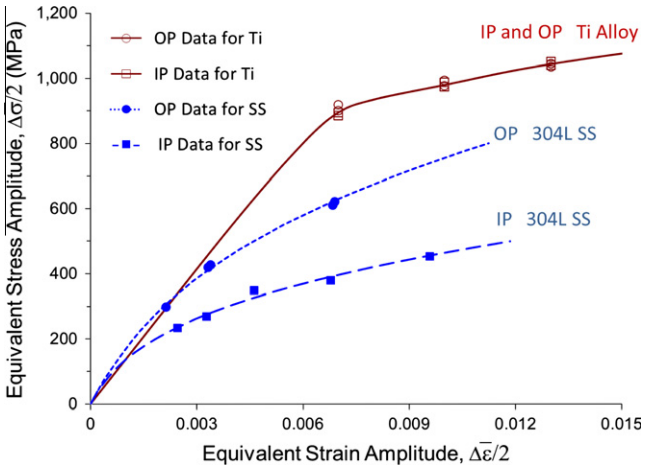

Fig. 4. Comparison of in-phase (IP) and 90° out-of-phase (OP) equivalent stress–strain data for Ti–6.5Al–3.4Mo (Ti) [17] and 304L stainless steel (SS) [18].

Shamsaei and Fatemi [18] found the value of cyclic hardening coefficient for a given material to depend on the material microstructure and hardness level. They also observed that cyclic hardening materials also exhibit non-proportional hardening under non-proportional loading, whereas cyclic softening materials do not typically display additional cyclic hardening. As both cyclic hardening and non-proportional hardening are associated with the stacking fault energy, they related the non-proportional cyclic hardening coefficient, α, to uniaxial monotonic and cyclic deformation properties and proposed the following empirical relation:

$$\alpha = 1.6\left(\frac{K}{K'}\right)^{2}\left(\frac{\Delta\varepsilon}{2}\right)^{2(n-n')} - 3.8\left(\frac{K}{K'}\right)\left(\frac{\Delta\varepsilon}{2}\right)^{(n-n')} + 2.2 \tag{2}$$

where K, K', n, and n' are uniaxial strength coefficient, cyclic strength coefficient, strain hardening exponent, and cyclic strain hardening exponent, respectively.

Experimental non-proportional cyclic hardening coefficients are compared with the values based on Eq. (2) for a wide variety of metallic materials in Fig. 5. This figure indicates a very good agreement between the different values. Therefore, this relation provides a simple approximation for the non-proportional cyclic hardening coefficient based on commonly available or easily obtainable uniaxial cyclic deformation material properties.

In general, there are two methodologies for estimation of stress response under general multiaxial loading; empirical formulations and constitutive models. Empirical models, such as in [16], relate the stress response of non-proportional loading directly to the strain path. Although these empirical models are simple, they can result in inaccurate stress response and, therefore, fatigue life [20].

Plasticity models which develop constitutive behavior based on continuum mechanics usually result in much better evaluation of stress response for complex loading, as compared to empirical models. The Armstrong–Frederick incremental plasticity model [21] has been shown in several studies, such as [22,23], as a proper basis for modeling various features of material behavior, including non-proportional hardening. This model considers the movement of the yield surface in deviatoric stress space by a nonlinear kinematic hardening rule, taking into account the strain memory effect by a recovery term.

Non-proportional cyclic hardening in constitutive models is taken into account by a non-proportionality parameter. Tanaka's non-proportionality parameter [24] has been reported to provide satisfactory evaluations for a variety of materials under various

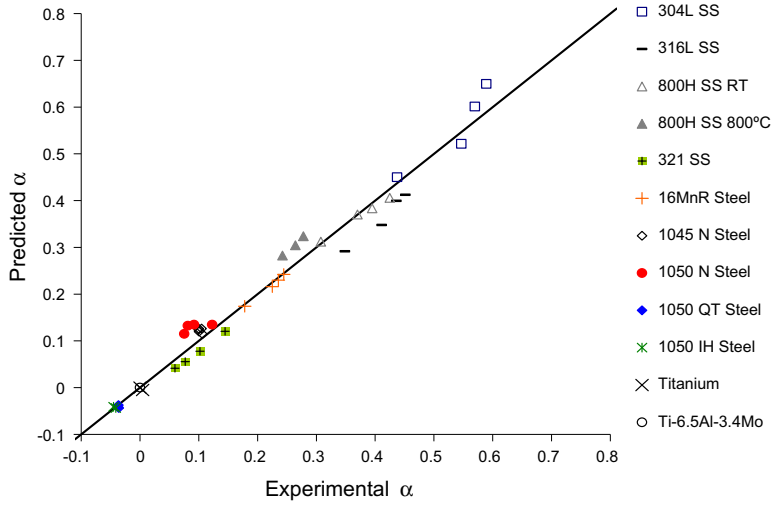

Fig. 5. Comparison of experimental and calculated values of non-proportional cyclic hardening coefficient, α, based on Eq. (2) [18].

non-proportional loading conditions, such as in [20,24,25]. This parameter is a function of the normalized plastic strain rate vector and the internal microstructure of material is represented by a fourth rank tensor in a 5-D plastic strain vector space.

Shamsaei et al. [20] have used Tanaka's non-proportionality parameter coupled with a simplified form of the Armstrong–Frederick incremental plasticity model which only requires five material constants (E, G, K', n', α) to estimate stress response for 304L stainless steel under several axial–torsion strain paths. In addition to in-phase and 90° out-of-phase strain paths shown in Fig. 6a, some star shape strain paths were also used, shown in Fig. 6b. One strain path consists of 360 proportional (in-phase) fully-reversed axial–torsion cycles with 1° increments starting from the pure axial cycle in $\gamma/\sqrt{3} - \varepsilon$ strain space (designated as FRI path). Another strain path also includes 360 proportional fully-reversed axial–torsion cycles, but applied in a random sequence (designated as FRR path). Therefore, the two paths are identical, except for the straining sequence. 304L stainless steel

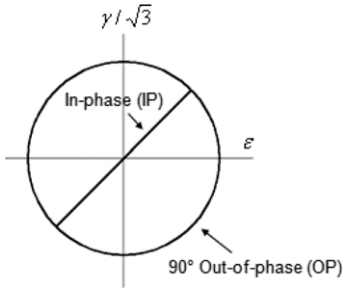

(a) In-phase (IP) and 90° out-of-phase (OP) strain paths.

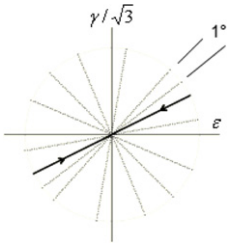

(b) In-phase cycles with incremental sequence (FRI) and with random sequence (FRR)

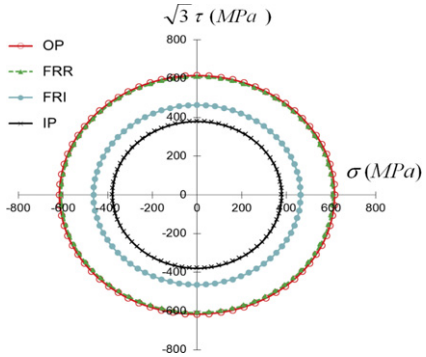

(c) IP, OP, FRI, and FRR experimental stress response at $\bar{\varepsilon}_a = 0.7\%$.

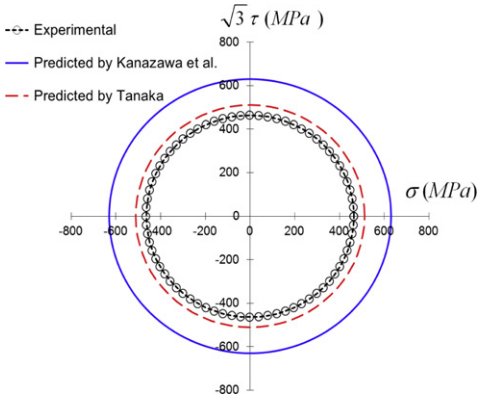

(d) Experimental and predicted stress boundary for FRI strain path at $\bar{\varepsilon}_a = 0.7\%$.

Fig. 6. (a) In-phase (IP) and 90° out-of-phase (OP) strain paths, (b) in-phase cycles with incremental sequence (FRI) and with random sequence (FRR), (c) IP, OP, FRI, and FRR experimental stress response, and (d) experimental and evaluated stress boundary for star shape path with gradual change in strain direction (FRI) at 0.7% equivalent strain amplitude for 304L stainless steel [20].

exhibited significant sensitivity to the straining sequence. In-phase loading with gradual change in strain direction (i.e. 1° increments), which activates the slip systems gradually but in all directions, results in some non-proportional hardening, as compared with in-phase loading. Star shape strain path composed of in-phase cycles but with random sequence resulted in significant non-proportional hardening and similar to 90° out-of-phase loading, as can be seen from Fig. 6c. This loading path causes cross hardening due to the interaction of the slip systems by activating intersecting slip bands within the material [20].

Tanaka's non-proportionality parameter coupled with the simplified form of the Armstrong–Frederick plasticity model results in stress response estimation within 12% of the experimental values for all the strain paths employed [26]. Kanazawa et al. empirical non-proportionality formulation, however, which considers the load non-proportionality as a factor of ellipticity of the circumscribed boundary around the strain path, results in identical stress response for the 90° out-of-phase and the star shape strain paths, regardless of straining sequence. This significantly over-estimates the stress for star path straining with gradual change in direction, as observed from Fig. 6d. Therefore, such empirical models cannot account for the progression of the cross hardening with change in the loading direction.

4. Damage parameters and life estimation

Classical yield criteria, such as von Mises distortion energy criterion, are commonly extended to multiaxial fatigue life estimations. Although these criteria may work for in-phase or proportional loading, they often under-estimate the typically observed shorter lives for out-of-phase or non-proportional loading. For example, for 90° out-of-phase sinusoidal axial–torsion loading with axial stress related to torsion stress by $\sqrt{3}$, von Mises equivalent stress remains constant during the loading cycle. This implies infinite life, regardless of the cyclic stress amplitudes. Therefore, such criteria are not generally appropriate for out-of-phase or non-proportional loading.

The shorter life of non-proportional loading is often attributed to additional hardening under such loading. However, materials without this hardening also typically exhibit shorter life under such a loading. Fig. 7 shows comparison of fatigue lives for in-phase and 90° out-of-phase loading for Ti–6.5Al–3.4Mo [17] and 1050 normalized (N) steel [27]. The Ti alloy is a material without non-proportional hardening (see Fig. 4), while 1050 N steel exhibits about 10–15% non-proportional cyclic hardening. As can be seen from Fig. 7, both materials show shorter life under out-of-phase loading at the same equivalent strain as in-phase loading, although the difference is larger for the 1050 N steel. von Mises criterion results in the same fatigue damage for both loadings and does not correlate the two sets of data for either material, as observed in Fig. 7.

Damage observations such as those presented in Fig. 1, and much work in the last 30 years suggest critical plane approaches are most reliable and robust for multiaxial fatigue life estimations. As discussed previously, these approaches reflect the physical nature of fatigue damage process. They consider specific plane(s) with maximum fatigue damage as the critical plane and are, therefore, also able to identify damage (i.e. crack) orientation. Critical plane approaches have been found to be applicable to both proportional and non-proportional loading conditions, and their applicability is not limited to metallic materials. For example, for elastomers, it has been shown that critical plane damage parameters are more accurate than scalar criteria such as von Mises, or the strain energy density criterion (SED), commonly used for elastomeric material life estimations [28,29]. Critical plane-based multiaxial fatigue criteria have also been shown to provide better life estimates than the

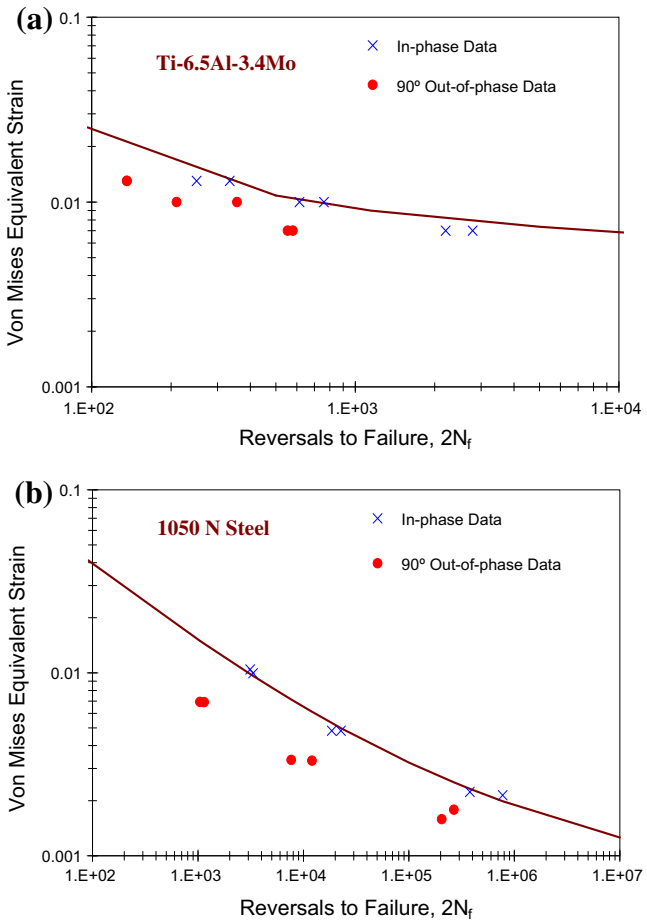

Fig. 7. In-phase and 90° out-of-phase fatigue data correlations by von Mises criterion for (a) Ti–6.5Al–3.4Mo [17] and (b) 1050 normalized (N) steel [27].

conventional criteria such as von Mises for many structural components, such as in welded joints (for example, in [30]).

Critical plane approaches are typically based on either the maximum shear plane or the maximum principal plane failure mode. They can be classified as stress-based, strain-based, and strain–stress-based or energy-based models. Stress-based critical plane models, such as Findley [31] model, may work well for high cycle fatigue (HCF), where plastic deformation is small or negligible. However, in many encountered fatigue problems, cyclic plastic deformation plays an important role in the damage process. This includes low cycle fatigue (LCF), notched components, and variable amplitude service loads containing overload cycles.

Strain-based critical plane models, such as Brown and Miller [10] model, are only based on strain terms. Although these models may apply to both low and high cycle fatigue, they cannot reflect constitutive behavior of the material. Therefore, effects of phenomena such as non-proportional cyclic hardening which can have a significant effect on fatigue life cannot be taken into account. In addition, such criteria typically identify two orthogonal critical planes, since both planes have the same shear and normal strains. However, cracking is usually observed on one preferred plane. For example, Fig. 1a shows that while many cracks exist, they are all on a single plane, rather than on two orthogonal planes. Thus, strain alone is not sufficient to identify the preferred critical plane and quantify fatigue damage.

Critical plane models with both stress and strain are, therefore, the most appropriate for general applicability to both LCF and HCF, and with the ability to capture material constitutive response un-

der non-proportional loading. Strain–stress-based critical plane models typically include a driving strain parameter and a secondary influencing stress parameter. Fatemi–Socie (FS) parameter [32] for shear failure mode materials (i.e. Fig. 2a) and Smith–Watson–Topper parameter [33] for tensile failure mode materials are examples of such critical plane models.The FS damage parameter is expressed as a function of the maximum shear strain amplitude, $\Delta\gamma_{max}/2$, and the maximum normal stress acting on the maximum shear strain plane over the cycle, $\sigma_{n,max}$, as:

$$\frac{\Delta\gamma_{max}}{2}\left(1+k\frac{\sigma_{n,max}}{\sigma_y}\right) \tag{3}$$

where σ_y is the material monotonic yield strength, and k is a material constant which can be found by fitting uniaxial fatigue data to torsion fatigue data. A distinct feature of this parameter is the coupling between the shear strain and the normal stress terms. Due to this coupling, shear strain alternation must be present for the normal stress term to cause fatigue damage. This prevents the normal stress term from contributing to fatigue damage, if the loading is not alternating (such as for static loading). Damage parameters without this coupling can incorrectly assign fatigue damage from static loads. Multiaxial fatigue data correlations and life estimations based on this parameter for a broad range of loadings, materials, and industrial applications have been shown by many investigators over the last two decades.

An example of damage distribution with plane orientation for in-phase and 90° out-of-phase axial–torsion loading with the same equivalent strain for Ti–6.5Al–3.4Mo [17] based on the FS parameter is shown in Fig. 8. A higher normal stress on the maximum shear plane for out-of-phase loading results in a higher damage value, as can be seen from Fig. 8, with the maximum damage on the 0° plane. Therefore, a shorter fatigue life is calculated as compared to in-phase loading, which corresponds with the experimental results (see Fig. 7). This is in spite of the fact that this Ti alloy does not exhibit non-proportional hardening under out-of-phase loading (see Fig. 4). For a material with non-proportional hardening, the normal stress term in Eq. (3) increases to a higher value, as compared to a material without this hardening. As Fig. 8 indicates, von Mises criterion results in the same damage for in-phase and 90° out-of-phase loadings, and on all planes.

Mean and/or residual stresses can also have a significant effect on fatigue behaviour. In multiaxial fatigue, the direction of the mean stress(s) with respect to the damage plane (critical plane) is important to be taken into account. For example, for a shear failure mode material, a tensile mean stress normal to the damage plane in Fig. 2a opens the crack, facilitating crack growth, resulting in shorter life. A compressive mean stress would have the opposite effect. However, a normal mean or static stress parallel to the shear critical plane in Fig. 2a may not have any influence on fatigue life. Therefore, the effect of the mean stress also depends on the material failure mode. Experimental evidence for these observations and discussions of mean or static normal and shear stresses are provided in [6,34]. The effect of a normal stress on the critical plane in the FS damage parameter is taken into account through the normal stress term, where the maximum normal stress $\sigma_{n,max}$ is composed of alternating and mean stress components.

A difficulty in life estimation is often lack of needed material fatigue properties. Roessle and Fatemi [35] proposed a method for estimation of the uniaxial strain-life curve as a function of Brinell hardness (HB). Several investigators have demonstrated the relative accuracy of this hardness method for a wide range of steels and hardness levels, for example in [36]. To enable calculation of multiaxial fatigue life in the absence of any fatigue data, a simple approximation for steels based on hardness is presented in [27]. This approximation combines the FS parameter with the Roessle–Fatemi hardness method:

$$\frac{\Delta\gamma_{max}}{2}\left(1+k\frac{\sigma_{n,max}}{\sigma_y}\right)=\left[A(2N_f)^{-0.09}+B(2N_f)^{-0.56}\right]\left[1+kC(2N_f)^{-0.09}\right] \tag{4}$$

where $k\approx 1$ and parameters A, B, and C are given in terms of Brinell hardness (HB) as:

$$A=\frac{5.53(HB)+293}{200,000},\quad B=\frac{0.48(HB)^2-731(HB)+286,500}{200,000},$$
$$C=\frac{1}{0.0022(HB)+0.382}$$

If not available, yield strength (σ_y) can also be estimated as a function of hardness [27].

Estimated fatigue lives based on Eq. (4) and only hardness as material property for several steels are compared with experimental lives in Fig. 9. This includes 1050 steel in normalized (N), quenched and tempered (QT), and induction-hardened (IH) conditions, two stainless steels, and Inconel 718 under a wide variety of loadings including axial–torsion and tension–tension, in-phase and out-of-phase, and with or without mean stress. In Fig. 9, 80% and 93% of the data fall within scatter bands of 3 and 5, respectively. It should also be mentioned that crack orientations for axial–torsion loadings of the 1050 steel at all hardness levels were found to be on the maximum shear plane [27]. Therefore, the use of shear-based multiaxial fatigue model is appropriate, in spite of the high hardness level of the IH condition at 565 HB.

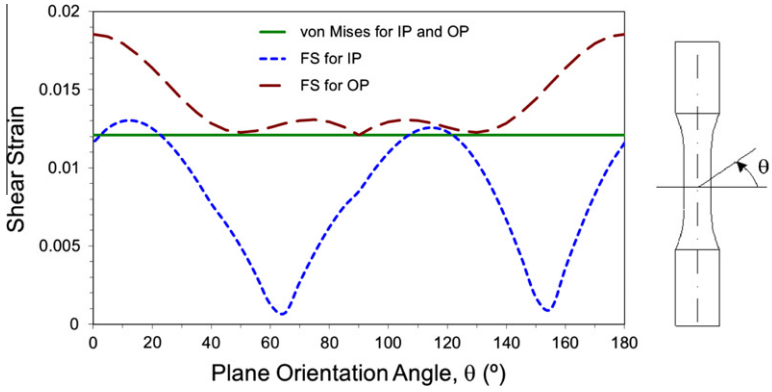

Fig. 8. Variation of von Mises and FS damage parameters with plane orientation for $\bar{\varepsilon}_a = 0.7\%$ of Ti–6.5Al–3.4Mo for in-phase (IP) and 90° out-of-phase (OP) axial–torsion loadings.

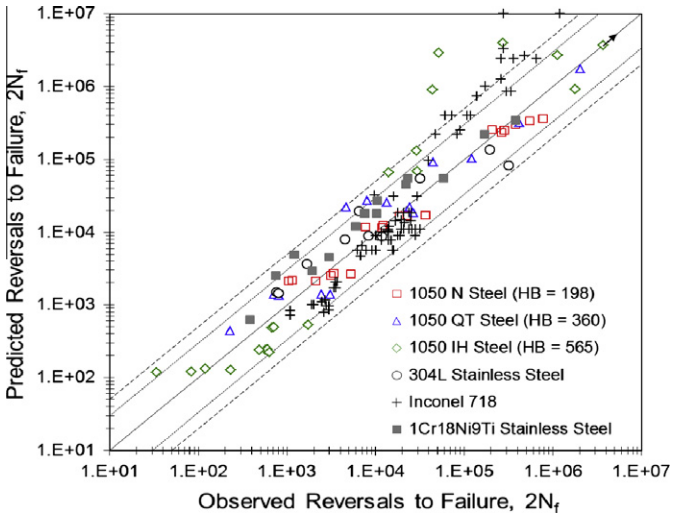

Fig. 9. Comparison of observed and estimated fatigue lives based on hardness for different materials under multiaxial loading conditions.

5. Variable amplitude loading and damage accumulation

To evaluate fatigue life under variable amplitude multiaxial loading, three components are essential: (1) a cycle counting method to identify cycles in the load history, (2) a multiaxial fatigue damage parameter to evaluate fatigue damage caused by each identified cycle, and (3) a cumulative damage rule to sum damage from all the counted cycles. Since a discussion of multiaxial damage parameters has already been presented, only cumulative damage and cycle counting are discussed in this section.

5.1. Cumulative damage

To compute the accumulated fatigue damage in variable amplitude loading, many nonlinear cumulative damage rules have been proposed. These nonlinear rules have been intended to address some of the shortcomings of the linear damage rule (LDR), such as load sequence and deformation history effects. However, LDR remains as the simplest and most commonly used cumulative damage rule [37].

Some of the shortcomings attributed to LDR in computing fatigue damage in the literature are not necessarily due to LDR, but due to the use of an unsuitable damage parameter. For example, even in uniaxial variable amplitude loading of materials with strong deformation history dependence such as stainless steel, it has been shown that LDR works very well if a damage parameter including both stress and strain terms is used to quantify damage from each loading cycle, rather than the commonly used *S–N* or strain–life curves [38]. This approach accounts for the deformation history dependence (i.e. constitutive response) of fatigue damage in each cycle damage calculation. However, while this approach addresses the deformation history dependence aspect in load sequence effects, it does not account for load amplitude dependence of load sequence effects which may also exist. High amplitude cycles followed by low amplitude cycles are usually more damaging than the reverse sequence, even for materials without constitutive behavior sensitivity to load sequence, such as some aluminum alloys [38].

In multiaxial fatigue, load path alteration can also affect fatigue life. For example, torsion followed by tension has been found to be more damaging than tension followed by torsion [39,40]. This has been explained [6] by torsion cycles nucleating small cracks on planes where subsequent tensile cycles can lead to their growth, while tensile cycles do not nucleate cracks on planes which can grow by torsion cycles. In LCF of Ti and its alloy presented in Fig. 10a, however, tension–torsion sequence (B1 block) is observed to be slightly more damaging than torsion–tension sequence (B2 block) [17].

In addition to axial (i.e. tension)–torsion and torsion–axial sequences, Fig. 10a also includes sequences of axial or torsion with 90° out-of-phase straining. Each part of the sequence for each material in this figure has identical equivalent strain amplitude (0.9% for Ti and 1% for its alloy) and all strain blocks are fully-reversed (i.e. no mean stress). As seen from Fig. 10a, shorter fatigue lives are observed by 90° out-of-phase loading followed by axial loading (B6 strain block), as compared to axial loading followed by 90° out-of-phase loading (B3 strain block). In addition, 90° out-of-phase followed by axial loading (B6 strain block) is more damaging than 90° out-of-phase followed by torsion loading (B4 strain block). It should be noted that, as Ti and its alloy are not sensitive to non-proportional hardening (see Fig. 4), this is not a factor in explaining the observed differences.

An important factor to consider when comparing the damage from each segment of the strain block is the parameter used for damage evaluation. Although each of the axial, torsion, and 90° out-of-phase segments of each block for each material in Fig. 10a has identical equivalent strain amplitude, the damage caused by each type of loading cycle is not the same. This is clearly observed

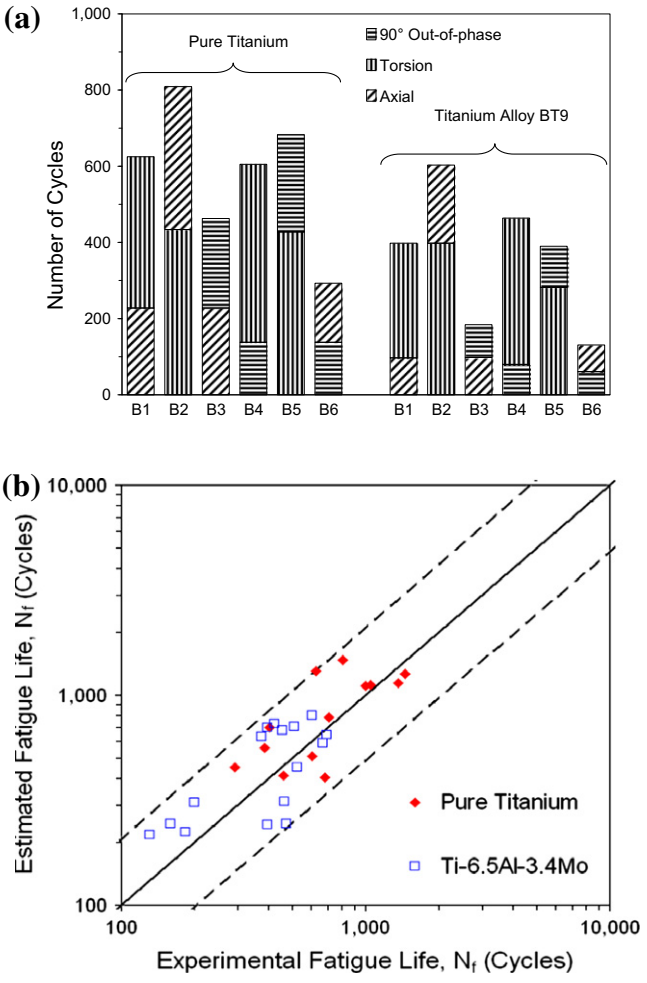

Fig. 10. (a) Observed fatigue lives for several strain block loadings of Ti and its alloy. (b) Comparison of observed and calculated fatigue lives by LDR and FS parameter [17].

from Fig. 11, where the damage value of each type of load in terms of the FS parameter is shown. The 90° out-of-phase loading causes a higher damage value than either axial or torsion loading. Placing 90° out-of-phase cycles at the beginning of a sequence (i.e. high-low loading) is, therefore, more damaging than placing them at the end of a sequence (i.e. low–high loading). This can explain the shorter live of the B6 strain block, as compared with those for the B3 strain block. Once small cracks nucleate under 90° out-of-phase cycles on or near 0° plane, which is the maximum damage plane (see Fig. 11), they can then grow faster under subsequent tensile cycles than under subsequent torsion cycles. This can explain the shorter lives of the B6 block, as compared with those for the B4 block.

Comparison of observed fatigue lives with estimated lives using LDR and FS parameter for various block loadings of Ti and its alloy are presented in Fig. 10b. This figure includes the loading blocks from Fig. 10a, as well as other blocks with several segments of axial, torsion, and 90° out-of-phase strain paths with the same equivalent strain, with each block repeated to failure [17]. To evaluate fatigue life, distribution of the damage parameter for each segment of loading is considered on different planes. Cumulative damage on each plane is then evaluated using LDR as the sum of damage caused by each segment of the load block. The plane with the greatest value of damage is chosen as the critical plane and fatigue life is calculated for this plane. Fig. 10b indicates the estimated fatigue lives to be within a factor of 2 of the experimental lives for both materials. Therefore, in spite of the fact that LDR does not account for some of the load sequence and load path alteration effects discussed with reference to the load blocks in Fig. 10a, it still results in reasonable life estimates, at least in the LCF region based on these data. Experimental results have also confirmed applicability of LDR for estimating fatigue life of elastomers under variable amplitude multiaxial loading [41].

5.2. Cycle counting method

In the case of general variable amplitude multiaxial loading, a cycle counting method is also required to identify different cycles within the load block. There are only a few proposals in the literature for cycle counting under multiaxial loading histories based on critical plane approaches. Bannantine and Socie [42] proposed a method based on the critical plane concept and rainflow cycle counting on the strain history as the main channel, mapped on the candidate planes within the material to determine the critical plane. In this method, rainflow cycle counting is performed on the shear strain history for shear failure mode materials, and on the normal strain history for tensile failure mode materials. Other components of the damage parameter (i.e. auxiliary channels), such as the maximum normal stress for FS parameter, are then determined for each counted cycle or reversal.

Wang and Brown [43] also proposed a cycle counting method based on rainflow and a modified von Mises equivalent strain. To overcome the sign problem in the von Mises equivalent strain and to be able to count out-of-phase cycles, they proposed a modified strain history by assigning a turning point at the greatest value of the equivalent strain. This method counts reversals and then discards them from the strain history. A new turning point is then defined and the process continues until all reversals are counted. Critical plane is then identified for each counted reversal, although the critical plane changes for each reversal. The method is analogous to rainflow counting an equivalent strain history.

The two aforementioned cycle counting methodologies have been examined under several discriminating axial–torsion strain paths with random and incremental changes in straining direction in [44]. These strain paths were applied to tubular stainless steel 304L and 1050 QT specimens. Two of these paths are shown in Fig. 6b as FRI and FRR strain paths. The von Mises criterion was found not to be suitable since it is overly non-conservative for fatigue life evaluations of variable amplitude strain blocks produced by these strain paths, even though the load block consists of only proportional or in-phase cycles. Satisfactory fatigue life estimations were obtained by either Bannantine–Socie (BS) or Wang–Brown (WB) cycle counting method, when coupled with the FS damage parameter and LDR. This is shown in Fig. 12 for the BS method and stainless steel 304L data, where the estimated lives are shown to be within a factor of two of the experimental fatigue lives. Crack orientation planes identified by using BS rainflow cycle counting method and FS critical plane parameter also correspond to the observed crack orientations.

Similarity of fatigue damage calculations based on the two cycle counting methods indicates that, although a proper cycle counting method to correctly identify cycles in a variable amplitude multiaxial load history can greatly affect the results, having a suitable damage parameter may be more essential. In spite of relative success, however, development of a reliable and robust cycle counting method for variable amplitude multiaxial loading remains a challenging problem. Related to this issue is the interaction between the components of the damage parameter, for example shear strain amplitude and maximum normal stress in FS parameter, for a counted cycle. Additional work is still needed to fully understand variable amplitude multiaxial loading effects in complex service load histories.

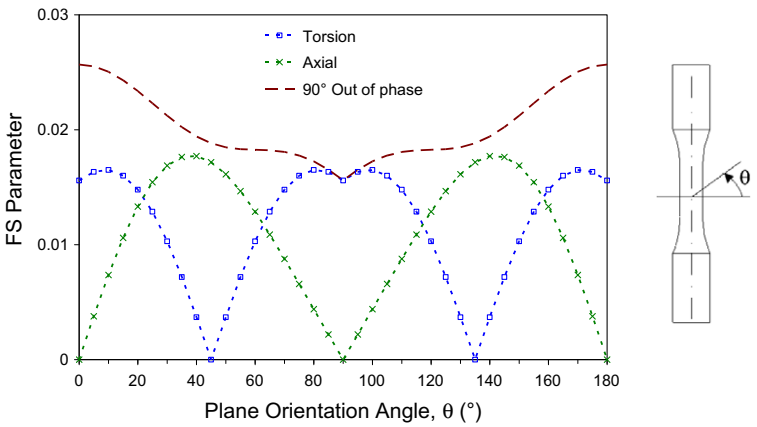

Fig. 11. Variation of the FS damage parameter with plane orientation for axial, torsion, and 90° out-of-phase loadings of Ti at $\bar{\varepsilon}_a = 0.9\%$ [17].

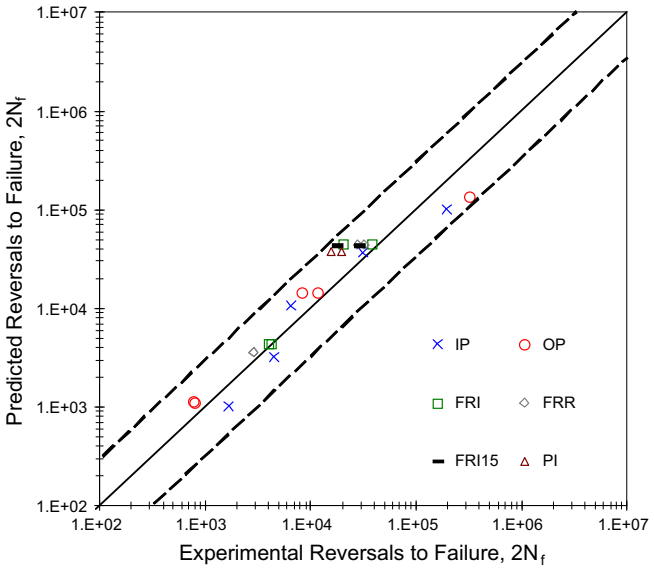

Fig. 12. Experimental and calculated fatigue lives of 304L stainless steel based on BS cycle counting method, FS critical plane approach, and linear cumulative damage rule [44].

6. Mixed-mode crack growth

Once micro-cracks nucleate, they often coalesce to form a dominant macro-crack, although still small in size (typically on the order of 1 mm). In some applications, a considerable portion of the total fatigue life is spent in macro-crack growth. Under multiaxial loads or combined stress states, the macro-crack can grow under mixed-mode loading conditions. As the crack often changes direction during its growth under mixed-mode loadings, both crack growth rate and crack growth direction are of importance in such applications [45]. In plate-type geometries, although cracks may form under mix-mode loading, they often turn into a mode I macro-crack after their early micro-crack growth period. Also, short or small cracks often exhibit different crack growth behaviour from that of long cracks. The difference is usually attributed to differences in plasticity-induced and roughness-induced closure mechanisms [46].

Several criteria have been used to predict crack growth direction under mixed-mode loading conditions. Maximum tangential stress (MTS) [47] and minimum strain energy density [48] criteria have been widely used because of their simplicity and support by experimental observations. According to the MTS criterion, the crack extends in a direction corresponding to the maximum tangential stress. According to the minimum strain energy density criterion, the crack grows in a direction along which the strain energy density factor reaches a minimum value. Observed crack growth directions and paths in plate specimens subjected to mixed-mode I and II loading have been found to be close to those based on the MTS criterion in [46].

To correlate fatigue crack growth rates under mixed-mode loading, equivalent strain and equivalent stress intensity factors have been used. A Paris-type equation is then used to calculate crack growth life. An equivalent strain-based intensity factor based on Eq. (3) can be adopted [49]:

$$\Delta K_{CPA} = G\Delta\gamma_{\max}\left(1 + k\frac{\sigma_{n,\max}}{\sigma_y}\right)\sqrt{\pi c} \tag{5}$$

where c is surface crack half-length. The parameter expressed by Eq. (5) has been shown to correlate small crack growth rate data for a wide variety of loading conditions of tubular specimens of 1045 N steel and Inconel 718 [49]. The loadings included axial, torsion, proportional and non-proportional axial–torsion with and without mean stress, as well as biaxial tension. An example of crack growth rate correlations with the parameter defined in Eq. (5) for in-phase and 90° out-of-phase axial–torsion loadings of solid round and tubular specimens made of 1045 and 1050 steels is shown in Fig. 13.

An equivalent stress intensity factor for mixed-mode loading can be based on the assumption that a fatigue crack grows when the sum of the absolute values of the crack tip displacements in a plastic strip reaches a critical value. Such an equivalent stress intensity factor range is expressed by [50]:

$$\Delta K_{eq} = \left[(\Delta K_I)^4 + 8(\Delta K_{II})^4 + \frac{8(\Delta K_{III})^4}{1-\nu}\right]^{0.25} \tag{6}$$

The J-integral concept, originally proposed for correlation of crack growth rates under mode I, was also extended to mixed-mode crack growth rate applications [51]. This approach was shown to correlate small crack growth rate data of Inconel 718 tubular specimens under axial, torsion, and proportional axial–torsion straining [51].

7. Summary

The large amount of experimental data and research over the last four decades has significantly advanced the understanding of multiaxial fatigue. However, due to the challenging nature of the problem, much additional research and development work is still needed for accurate and reliable multiaxial fatigue life estimation. This overview paper has discussed several important issues related to multiaxial fatigue. Some simple approximations for life estimations under multiaxial loads have also been presented.

Systematic investigation of cracking behavior under multiaxial loading indicates that cracks nucleate and grow on preferred planes. The preferred orientation depends on the material and the state of loading. These observations have provided the physical basis for critical plane approaches to multiaxial fatigue. For shear

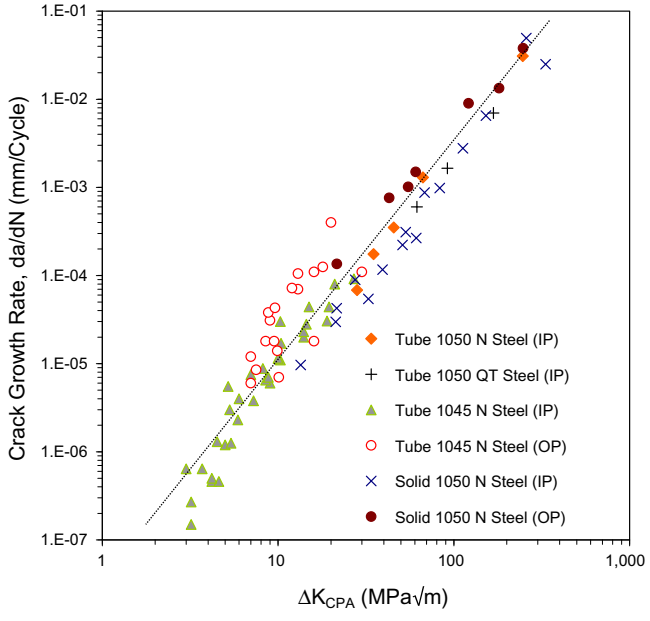

Fig. 13. Crack growth rate data correlations with an equivalent strain-based intensity factor for in-phase (IP) and 90° out-of-phase (OP) axial–torsion loadings of solid round and tubular specimens made of 1045 and 1050 normalized (N) and quenched and tempered (QT) steels.

cracking mechanism materials, the stress normal to the cracking plane has a secondary influence. A tensile normal stress opens the crack and reduces crack closure, resulting in decreased fatigue life, while a compressive normal stress has the opposite effect.

Some materials exhibit additional cyclic hardening under non-proportional loading conditions. This hardening is attributed to the change in crystallographic slip planes due to the rotation and intersection of maximum shear planes. The level of non-proportional hardening depends on the shape, sequence, and amplitude of the load path, as well as the microstructure of the material. Sensitivity of a material to non-proportional cyclic loading is usually determined by non-proportional cyclic hardening coefficient.

It has been found that cyclic hardening materials also exhibit non-proportional hardening under non-proportional loading, whereas cyclic softening materials do not typically display additional cyclic hardening. As both cyclic hardening and non-proportional hardening are associated with the stacking fault energy, the non-proportional cyclic hardening coefficient has been related to uniaxial monotonic and cyclic deformation properties. A simple approximation for the non-proportional multiaxial cyclic hardening coefficient has been presented based on commonly available or easily obtainable uniaxial cyclic deformation material properties.

Plasticity models which develop constitutive behavior based on continuum mechanics usually result in much better evaluations of stress response for complex multiaxial loading, as compared to empirical models. While non-proportional cyclic hardening in constitutive models is taken into account by a non-proportionality parameter, empirical non-proportionality formulations consider the load non-proportionality as a function of the circumscribed boundary around the strain path. Such empirical models, although simple to use, cannot account for the progression of the cross hardening with change in the loading direction and may result in significant errors in estimated stresses and, therefore, fatigue life.

Classical yield criteria, such as von Mises distortion energy criterion, are commonly extended to multiaxial fatigue life estimations. Although these criteria may work for in-phase or proportional loading, they often under-estimate the typically observed shorter lives for out-of-phase or non-proportional loading. The shorter life under non-proportional loading is often attributed to non-proportional hardening. However, materials without this hardening also typically exhibit shorter life under such a loading. Classical criteria, such as von Mises equivalent strain, cannot represent this behavior and should not be used for non-proportional loading.

Damage observations and much work in the last 30 years suggest critical plane approaches which reflect the physical nature of fatigue damage process are most reliable and robust for multiaxial fatigue life estimations. These approaches consider specific plane(s) with maximum fatigue damage as the critical plane and are, therefore, also able to predict damage (i.e. crack) orientation. Critical plane models with both stress and strain terms are the most appropriate due to their general applicability to both LCF and HCF, and for their ability to capture material constitutive response under non-proportional loading. The Fatemi–Socie (FS) model for shear failure mode materials is an example of such a critical plane model.

A difficulty in multiaxial fatigue life estimation is often lack of needed material fatigue properties. To enable calculation of multiaxial fatigue life in the absence of any fatigue data, a simple approximation for steels based on hardness has been presented. Estimated fatigue lives based on only hardness as material property have been shown to compare favorably with experimental lives for several steels and under a wide variety of loading conditions.

In addition to a proper fatigue damage model, a cycle counting method to identify cycles in a load history, and a cumulative damage rule to sum damage from all the counted cycles are needed for evaluating fatigue life under variable amplitude multiaxial loading. Although many nonlinear cumulative damage rules have been proposed, LDR remains as the simplest and most commonly used cumulative damage rule. Some of the shortcomings attributed to LDR in computing fatigue damage in the literature are not necessarily due to LDR, but are due to the use of an unsuitable damage parameter. In multiaxial fatigue, load path alteration can also affect fatigue life.

In the general case of variable amplitude multiaxial loading, a cycle counting method is also required to identify different cycles within the load block. There are only a few proposals in the literature for cycle counting under multiaxial loading histories based on critical plane approaches. In spite of relative success, however, development of a reliable and robust cycle counting method for variable amplitude multiaxial loading remains a challenging problem.

Mixed-mode crack growth can constitute a significant portion of the total fatigue life under multiaxial loads or combined stress states. As the crack often changes direction during its growth under mixed-mode loadings, both crack growth rate and crack growth direction are important. Maximum tangential stress and minimum strain energy density criteria have been widely used to evaluate crack growth direction because of their simplicity and support by experimental observations. To correlate fatigue crack growth rates under mixed-mode loading, equivalent strain and equivalent stress intensity factors have been used.

In plate-type geometries, although cracks may form under mix-mode loading, they often turn into a mode I macro-crack after their early crack growth period. In cylindrical-type geometries, cracks often form and grow in shear (mode II) in the short crack regime. An equivalent strain-based intensity factor based on extension of the FS parameter has been shown to correlate crack growth rate data for several steels under in-phase and out-of-phase axial–torsion loading conditions. Short or small cracks may exhibit a crack growth behaviour different from that of long cracks and the difference is usually attributed to differences in plasticity-induced and roughness-induced closure mechanisms.

References

[1] Lanza G. Strength of shafting subjected to both twisting and bending. Trans ASME 1886;8:130–44.
[2] Gough HJ, Pollard HV. The strength of metals under combined alternating stresses. Proc Inst Mech Eng 1935;131:3–103.
[3] Gough HJ. Engineering steels under combined cyclic and static stresses. J Appl Mech 1950;50:113–25.
[4] Sines G. Behavior of metals under complex static and alternating stresses. In: Sines G, Waisman JL, editors. Metal fatigue. New York: McGraw-Hill; 1959. p. 145–69.
[5] Findley WN. A theory for the effect of mean stress on fatigue of metals under combined torsion and axial load or bending. J Eng Ind 1959:301–6.
[6] Socie DF, Marquis GB. Multiaxial fatigue. Society of Automotive Engineers, Inc.; 2000.
[7] Hua CT, Socie DF. Fatigue damage in 1045 steel under variable amplitude biaxial loading. Fatigue Fract Eng Mater Struct 1985;8:101–14.
[8] Bannantine JA, Socie DF. Observations of cracking behavior in tension and torsion low cycle fatigue. In: Solomon HD, Halford GR, Kaisand LR, Leis BN, editors. ASTM symposium on low cycle fatigue, vol. 942. ASTM STP; 1988. p. 899–921.
[9] Brown MW, Miller KJ. Initiation and growth of cracks in biaxial fatigue. Fatigue Eng Mater Struct 1979;1:231–46.
[10] Brown MW, Miller KJ. High temperature biaxial fatigue of two steels. Fatigue Eng Mater Struct 1979;1:217–29.
[11] Mars WV, Fatemi A. Nucleation and growth of small fatigue cracks in filled natural rubber under multiaxial loading. J Mater Sci 2006;41:7324–32.
[12] Shamsaei N, Fatemi A. Deformation and fatigue behaviors of case-hardened steels in torsion: experiments and predictions. Int J Fatigue 2009;31:1386–96.
[13] Cryderman R, Shamsaei N, Fatemi A. Effects of continuous cast section size on torsion deformation and fatigue of 1050 steel shafts. J Mater Process Technol 2011;211:66–77.

[14] Taira S, Inoue T, Yoshida S. Low cycle fatigue under multiaxial stress in the case of combined cyclic tension compression and cyclic torsion out-of-phase at elevated temperature. In: Proceedings of 11th Japan congress on materials research, vol. 5; 1968. p. 60–5.
[15] Lamba HS, Sidebottom OM. Cyclic plasticity for nonproportional paths: part 1 – cyclic hardening, erasure of memory, and subsequent strain hardening experiments: part 2 – comparison with prediction of three incremental plasticity models. ASME J Eng Mater Technol 1978;100:96–103.
[16] Kanazawa K, Miller KJ, Brown MW. Cyclic deformation of 1% Cr–Mo–V steel under out-of-phase loads. Fatigue Eng Mater Struct 1979;2:217–28.
[17] Shamsaei N, Gladskyi M, Panasovskyi K, Shukaev S, Fatemi A. Multiaxial fatigue of titanium including step loading and load path alteration and sequence effects. Int J Fatigue 2010;32:1862–74.
[18] Shamsaei N, Fatemi A. Effect of microstructure and hardness on non-proportional cyclic hardening coefficient and predictions. J Mater Sci Eng A 2010;527:3015–24.
[19] Sonsino CM, Grubisic V. Fatigue behavior of cyclically softening and hardening steels under multiaxial elastic–plastic deformation. In: Miller KJ, Brown MW, editors. ASTM symposium of multiaxial fatigue, vol. 853. ASTM STP; 1985. p. 586–605.
[20] Shamsaei N, Fatemi A, Socie DF. Multiaxial cyclic deformation and non-proportional hardening employing discriminating load paths. Int J Plasticity 2010;26:1680–701.
[21] Armsrong PJ, Frederick CO. A mathematical representation of the multiaxial Bauschinger effect. CEGB Report, RD/B/N731. Berkeley Nuclear Laboratories; 1966.
[22] Jiang YY, Kurath P. Characteristics of the Armstrong–Frederick type plasticity models. Int J Plasticity 1996;12(3):387–415.
[23] Chaboche JL. A review of some plasticity and viscoplasticity constitutive theories. Int J Plasticity 2008;24:1642–93.
[24] Tanaka E. A nonproportionality parameter and a cyclic viscoplastic constitutive model taking into account amplitude dependence and memory effects of isotropic hardening. Eur J Mech A Solids 1994;13:155–73.
[25] Zhang JX, Jiang YY. Constitutive modeling of cyclic plasticity deformation of a pure polycrystalline copper. Int J Plasticity 2008;24:1890–915.
[26] Shamsaei N, Fatemi A, Socie DF. Multiaxial deformation and fatigue behaviors under discriminating strain paths. In: 9th International conference on multiaxial fatigue and fracture (ICMFF9), Parma, Italy, 2010.
[27] Shamsaei N, Fatemi A. Effect of hardness on multiaxial fatigue behavior and some simple approximations for steels. Fatigue Fract Eng Mater Struct 2009;32:631–46.
[28] Mars WV, Fatemi A. Multiaxial fatigue of rubber, part I: equivalence criteria and theoretical aspects. Fatigue Fract Eng Mater Struct 2005;28: 515–22.
[29] Mars WV, Fatemi A. Multiaxial fatigue of rubber, part II: experimental observations and life predictions. Fatigue Fract Eng Mater Struct 2005;28:523–38.
[30] Carpinteri A, Spagnoli A, Vantadori S. Multiaxial fatigue life estimation in welded joints using the critical plane approach. Int J Fatigue 2009;31:188–96.
[31] Findley WN. Modified theory of fatigue failure under combined stress. Proc Soc Experiment Stress Anal 1956;14(1):35–46.
[32] Fatemi A, Socie DF. A critical plane approach to multiaxial fatigue damage including out-of-phase loading. Fatigue Fract Eng Mater Struct 1988;11(3):149–65.
[33] Smith RN, Watson PP, Topper TH. A stress–strain parameter for the fatigue of metals. J Mater 1970;5(4):767–78.
[34] Fatemi A, Kurath PP. Multiaxial fatigue life prediction under the influence of mean stresses. ASME J Eng Mater Technol 1988;110:380–8.
[35] Roessle ML, Fatemi A. Strain-controlled fatigue properties of steels and some simple approximations. Int J Fatigue 2000;22:495–511.
[36] Kim KS, Chen X, Han C, Lee HW. Estimation methods for fatigue properties of steels under axial and torsional loading. Int J Fatigue 2002;24:783–93.
[37] Fatemi A, Yang L. Cumulative fatigue damage and life prediction theories: a survey of the state of the art for homogeneous materials. Int J Fatigue 1998;20:9–34.
[38] Colin J, Fatemi A. Variable amplitude cyclic deformation and fatigue behaviour of stainless steel 304L including step, periodic, and random loadings. Fatigue Fract Eng Mater Struct 2010;33:205–20.
[39] Miller KJ. Materials science perspective of metal fatigue resistance. Mater Sci Technol 1993;9:453–62.
[40] Harada S, Endo T. On the validity of Miner's rule under sequential loading of rotating bending and cyclic torsion. In: Kussmaul K, McDiarmid D, Socie D, editors. Fatigue under biaxial and multiaxial loading. London: European Structural Integrity Society, ESIS Publication 10, Mechanical Engineering Publications; 1991. p. 161–78.
[41] Harbour RJ, Fatemi A, Mars WV. Fatigue life analysis and predictions in NR and SBR under variable amplitude and multiaxial loading conditions. Int J Fatigue 2008;30:1231–47.
[42] Bannantine JA, Socie DF. A variable amplitude multiaxial fatigue life prediction model. In: Kussmaul K, McDiarmid D, Socie D, editors. Fatigue under biaxial and multiaxial loading. London: European Structural Integrity Society, ESIS Publication 10, Mechanical Engineering Publications; 1991. p. 35–51.
[43] Wang CH, Brown MW. Life prediction techniques for variable amplitude multiaxial fatigue – part 1: theories. ASME J Eng Mater Technol 1996;118:367–70.
[44] Shamsaei N, Fatemi A, Socie DF. Multiaxial fatigue evaluation using discriminating strain paths. Int J Fatigue 2011;33:597–609.
[45] Qian J, Fatemi A. Mixed-mode fatigue crack growth: a literature survey. Eng Fract Mech 1996;55:969–90.
[46] Zhang H, Fatemi A. Short fatigue crack growth behavior under mixed-mode loading. Int J Fract 2010;165:1–19.
[47] Erdogan F, Sih GC. On the crack extension in plates under plane loading and transverse shear. ASME J Basic Eng 1963;85:519–25.
[48] Sih GC. Strain energy density factor applied to mixed-mode crack problems. Int J Fract 1974;10:305–21.
[49] Reddy SC, Fatemi A. Small crack growth in multiaxial fatigue. In: Mitchell MR, Landgraf RW, editors. ASTM symposium in advances in fatigue lifetime predictive techniques, vol. 1122. ASTM STP; 1992. p. 569–85.
[50] Tanaka K. Fatigue crack propagation from a crack inclined to the cyclic tensile axis. Eng Fract Mech 1974;6:493–507.
[51] Hoshide T, Socie DF. Mechanics of mixed-mode small fatigue crack growth. Eng Fract Mech 1987;26:841–50.